Talanta 82 (2010) 1725–1732

Contents lists available at ScienceDirect

Talanta

journal homepage: www.elsevier.com/locate/talanta

An enzyme-free highly glucose-specific assay using self-assembled aminobenzene boronic acid upon polyelectrolytes electrospun nanofibers-mat

Ashutosh Tiwari[a,b,*], Dohiko Terada[a], Chiaki Yoshikawa[c], Hisatoshi Kobayashi[a,d,*]

[a] Biomaterials Center, National Institute for Materials Science, 1-2-1 Sengen, Tsukuba, Ibaraki 350047, Japan
[b] JSPS, Sumitomo-Ichibancho Bldg. 6 Ichibancho, Chiyoda-ku, Tokyo 1028471, Japan
[c] International Center for Materials Nanoarchitectonics, 1-2-1 Sengen, Tsukuba, Ibaraki 350047, Japan
[d] JST CREST, Kawaguchi, Saitama 3320012, Japan

ARTICLE INFO

Article history:
Received 20 July 2010
Received in revised form 27 July 2010
Accepted 27 July 2010
Available online 6 August 2010

Keywords:
Self-assembly
Polyelectrolyte
Nanofibers-mat
Boronic acid
Glucose sensors

ABSTRACT

A highly selective enzyme-free amperometric glucose sensor based on electrostatic self-assembling of 3-aminobenzene boronic acid (ABBA) onto a poly(styrene-*co*-acrylamide)/polystyrene sulfonic acid (PSA/PSSA) electrospun nanofibers-mat was investigated. Emerging ability of phenylboronic acid to bind with the diols of sugars has been extended for rapid response of glucose with a pH-sensitive redox mediator, hematein natural dye. ABBA was adsorbed on the PSA/PSSA nanofibers-mat/Pt-disc electrode that resulted in an ABBA/PSA/PSSA glucose active electrode. The interaction of ABBA onto the PSA/PSSA nanofibers-mat/Pt-disc electrode was characterized with Fourier transform infrared spectroscopy (FT-IR), ζ-potential, scanning electron microscopy (SEM), contact angle and cyclic voltammetry (CV) measurements. The prepared enzyme-free sensor exhibited a fast amperometric response, i.e., about 4 s and linearity ranging from 0.75 to 14 mM to glucose with a sensitivity of 0.987 $\mu A\,mM^{-1}\,cm^{-2}$. Compared to other types of glucose biosensors viz. use glucose oxidase as sensing elements, present glucose sensor offers basic advantages including ease of fabrication, high affinity-selectivity to the glucose upon the electrode surface and quick response.

1. Introduction

Diabetes mellitus is a major worldwide public health problem associated with glucose metabolism. Typically, it is reflected by lower or higher than normal range of glucose concentration from 4.4 to 6.6 mM in the blood [1,2]. Indeed, there is a fairly need to develop efficient, selective and cheap glucose sensors. Lately, phenylboronic acids have gain considerable attention as a promising alternative to the well-known glucose oxidase enzyme technology which lean to be complex and expensive [3,4]. Boronic acids are competent to react with glucose and form cyclic ester. For glucose sensing a range of physical transducers such as electrochemical, optical, etc. can use to translate the glucose-recognition event into a corresponding physical signal. Among them, electrochemical biosensors have been considered as excellent analytical tool for rapid and inexpensive glucose-recognition [5,6].

In this paper, we report an enzyme-free glucose-responsive electrospun nanofibers-mat using amphiphilic poly(styrene-*co*-acrylamide)/polystyrene sulfonic acid (PSA/PSSA) polyelectrolyte containing self-assembled 3-aminobenzene boronic acid (ABBA) as a glucose-sensitive moiety. Since, esterification of boronic acid with glucose is pH dependent process, therefore glucose-sensing properties are significantly quick near pK_a of used boronic acid derivatives, i.e., normally located between 7.5 and 9.5 [7]. In this respect, ABBA containing electrospun polyelectrolyte nanofibers-mat having ionizable structural properties make them extremely attractive for the task of glucose sensor in general and electrochemical detection in particular. It is well established that the performance of electrochemical sensors greatly depends on the physicochemical properties of the electrode materials and concentration of sensing elements on the electrode surface [8,9]. As a result, the use of porous nanofibers-mat to fabricate sensor is one of the most exciting approach because surface topology affect for occasion the wetting behavior as well as large surface area available for adsorption of ABBA. We have found that materials can also be tailored in the molecular scale in order to achieve various desirable sensing properties [10–13]. Many attempts have been made to fabricate glucose biosensor with enzyme technology [14–21] however, these approaches were based on enzyme self-assembly and due to bulky enzyme they may only offer limited available surface

* Corresponding authors at: Biomaterials Center, National Institute for Materials Science, 1-2-1 Sengen, Tsukuba, Ibaraki 350047, Japan. Tel.: +81 29 860 4495; fax: +81 29 859 2247.
E-mail addresses: tiwari.ashutosh@nims.go.jp (A. Tiwari), kobayashi.hisatoshi@nims.go.jp (H. Kobayashi).

0039-9140/$ – see front matter © 2010 Elsevier B.V. All rights reserved.
doi:10.1016/j.talanta.2010.07.078

area on the electrode, which can compromise the performance of the biosensors.

Meanwhile, polyelectrolytes have played an increasingly important role for biosensor applications [22,23]. Polyelectrolytes can (1) provide a stable surface for the adsorption of ABBA without compromising their chemical activities; and (2) permit direct electron transfer from the electro-active molecules to the porous PSA/PSSA nanofibers-mat electrode, thereby enhancing the electrochemical sensing ability. For example, Geest et al. systematically studied the new photoelectronic glucose-recognition system that used poly(acrylamidophenylboronic acid)-*co*-poly(methyl aminoethyl acrylate)/polystyrene sulfonate polyelectrolyte capsules [24]. Moreover, this study also indicates that polyelectrolyte macromolecules can generally retain their pH-responsive behavior and ionic activity even after adsorption of boronic acid.

This study investigates the feasibility of using self-assembled ABBA containing PSA/PSSA polyelectrolyte electrospun nanofibers-mat for a potential enzyme-free glucose-sensing application. Amphiphilic PSA/PSSA polyelectrolyte electrospun nanofibers-mat is particularly attractive for sensor fabrication because they can be prepared under ambient conditions and they also have large surface-to-volume ratio, tunable porosity, pH-responsive groups, high chemical inertness, etc. while experiencing negligible swelling in aqueous medium. This novel enzyme-free glucose assay offers a relatively high selectivity, sensitivity, and fast response time.

2. Materials and methods

2.1. Materials

Styrene (Wako, Osaka, Japan, 98%), sodium *p*-styrenesulfonate (Wako, Osaka, Japan, 98%), potassium peroxodisulfate ($K_2S_2O_8$, Wako, Osaka, Japan, 99%,), 3-aminobenzene boronic acid (ABBA, Alfa Aesar, MA, USA, 98%), hematein (Waldeck, Tokyo, Japan, 99%), D-glucose (Wako, Osaka, Japan, 98%), L-ascorbic acid (Sigma, PA, USA, 95%), DL-malic acid (SAJ, Tokyo, Japan, 99%), L-alanine (Kabu, Tokyo, Japan, 99%), L-proline (Wako, Osaka, Japan, 99%) and sodium chloride (Wako, Osaka, Japan, 99%, NaCl) were used without further purification. All supplementary chemicals were of analytical grade and solutions were prepared with mili-Q water. In order to eliminate the inhibitor from styrene monomer, styrene was washed three times with a 10% (w/v) NaOH aqueous solution followed by rinsing with mili-Q water.

2.2. Synthesis of polyelectrolytes

Amphiphilic polyelectrolyte, i.e., the polycationic and polyanionic polystyrenes were prepared separately via surfactant-free emulsion polymerization technique [25]. First, the cationic polystyrene random copolymer was secured with polyacrylamide. Next, anionic amphiphilic polystyrene was synthesized by homopolymerization of sodium *p*-styrenesulfonate monomers.

2.3. Synthesis of poly(styrene-co-acrylamide)

To prepare the poly(styrene-*co*-acrylamide) (PSA), styrene (15 mM), acrylamide (10 mM) and $K_2S_2O_8$ (14 mM) were mixed with 12 mL mili-Q water in a 25 mL capped reaction tube. Before start the reaction, the reaction tube was completely deoxygenated using N_2 gas bubbling. Next, the polymerization reaction was carried out under ultrasound irradiation (cf., 38 kHz) water bath at 60 °C for 2 h and at the end of reaction, a viscous solution was yielded. Typically, PSA was separated from unreacted styrene monomer and polystyrene homopolymer by pouring the viscous solution into a large quantity of toluene. The copolymer was separated from polyacrylamide and acrylamide by precipitating the resulting solution with methanol and water (7:3, v/v) mixture. Finally, a white, fluffy solid of PSA was obtained after vacuum-drying at room temperature. PSA yield (%) = 85.5; FT-IR (KBr, cm^{-1}): 3433 (ν_{N-H}), 2920 (ν_{C-H}), 2840 (ν_{C-H}), 1638 ($\nu_{C=O}$), 951, 770, 684 (δ_{C-H}); ^{1}H NMR (DMSO-d_6/CD_3Cl, TMS): δ 1.4 (d, –C–H_2), δ 1.6 (s, –C–H), δ 1.8 (s, –C–H), δ 2.4 (t, –C–H), δ 6.5 (s, –C–H), δ 7.0 (s, –C–H); M_w (DMF with 10 mM LiCl) = 163 kDa.

2.4. Synthesis of polystyrene sulfonic acid

The reaction was carried out in 25 mL reaction tube capped with stopper. The reaction tube was charged with 15 mL mili-Q water and 18 mM sodium *p*-styrenesulfonate. After complete dissolution of *p*-styrenesulfonate in water, 15 mM $K_2S_2O_8$ was added. The reaction tube was capped with a rubber septum followed by purging of N_2 gas for 10 min. The reaction mixture was then placed in water bath at 60 °C under ultrasound irradiation (cf., 38 kHz), and the polymerization was carried out with constant sonication for 3 h. At the end of reaction, the reaction mixture became thick and white. After that, the polymer solution was placed into a large quantity of methanol and water (6:4, v/v) mixture. The slow precipitation process was carried out for 2–3 days. The recovered precipitate was washed several times with water to ensure removal of all salts and unreacted monomers from the product. The polystyrene sulfonic acid (PSSA) was dried under vacuum at room temperature. PSSA yield (%) = 93.7; FT-IR (KBr, cm^{-1}): 3184 (ν_{O-H}), 2929 (ν_{C-H}), 2810 (ν_{C-H}), 1604 (ν_{C-C}), 1187 ($\nu_{S=O}$), 1039 ($\delta_{S=O}$), 835, 770, 697 (δ_{C-H}); M_w (THF) = 399 kDa.

2.5. Fabrication of electrospun nanofibers-mat

PSA (5.8 g, M_w 163 kDa) and PSSA (2.9 g, M_w 399 kDa) were dissolved in 100 mL of 1,1,1,3,3,3-hexafluoro-2-propanol/*N*,*N*-dimethylformamide (9.5:0.5, w/w) mixture. Both solutions were mixed under gentle stirring at room temperature. The electrospun nanofibers-mat was fabricated using conventional needle-plate electrospinning setup [26]. The voltage, flow rate, humidity and distance from needle to plate were 9.3 kV, 0.08 mL/h, <10% and 27 cm, respectively. A randomly oriented nonwoven net was collected onto ground aluminum foil and before further study; nanofibers-mat was kept under vacuum for 15 h at room temperature. FT-IR (ATR, cm^{-1}): 3398 (ν_{N-H}), 3186 (ν_{O-H}), 2920 (ν_{C-H}), 2844 (ν_{C-H}), 1658 ($\nu_{C=O}$), 1605 (ν_{C-C}), 1184 ($\nu_{S=O}$), 1042 ($\delta_{S=O}$), 836, 773, 670 (δ_{C-H}).

2.6. Self-assembly of ABBA onto PSA/PSSA electrospun nanofibers-mat

PSA/PSSA electrospun nanofibers-mat with a mean thickness of ~5 μm was used as a self-sacrificial template. The self-assembling of 100 mM ABBA onto PSA/PSSA nanofibers-mat was preferably performed by the physical adsorption technique. After adsorption steps, the mat was rinsed with phosphate buffer saline (PBS) at physiological pH in order to remove the excess unbound ABBA and then, kept under vacuum for 10 h at room temperature. FT-IR (ATR, cm^{-1}): 3390 (ν_{N-H}), 3189 (ν_{O-H}), 2921 (ν_{C-H}), 2845 (ν_{C-H}), 1657 ($\nu_{C=O}$), 1604 (ν_{C-C}), 1349 (ν_{B-O}), 1172 ($\nu_{S=O}$), 1038 ($\delta_{S=O}$), 839, 770, 674 (δ_{C-H}).

2.7. Apparatus and instrumentation

All the electrochemical measurements were executed using ALS/HCH 852CB electrochemical analyzer. A three electrode system was secured with a modified platinum disc electrode (Pt-electrode, outer diameter, OD: 6 mm, inner diameter, ID: 3 mm and PTE: 6 mm × 3 mm), platinum wire, and Ag/AgCl (saturated KCl) as a

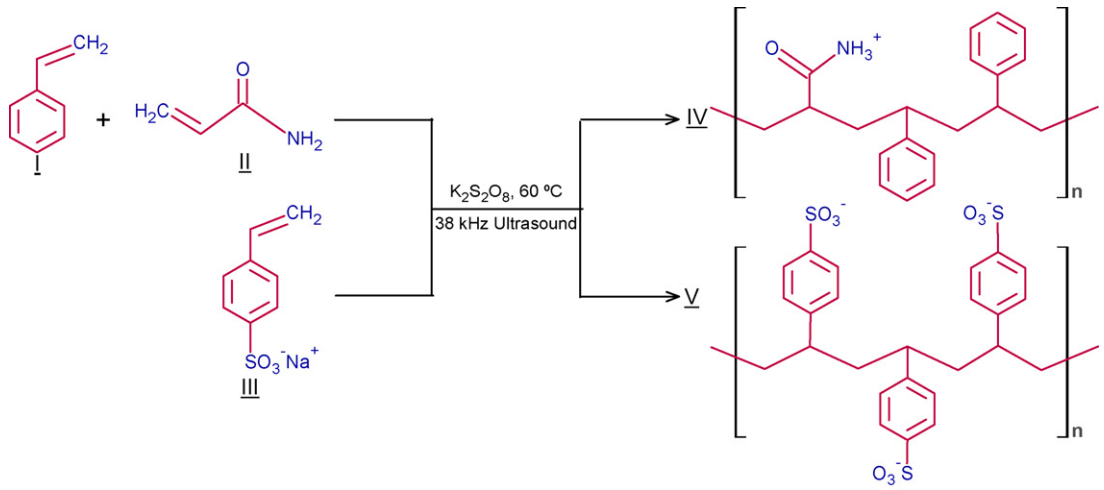

Fig. 1. Chemical illustrations of PSA (IV) and PSSA (V) polyelectrolytes synthesis.

working, counter and reference electrodes, respectively. A 50 mM PBS of pH 7.4 containing 1 M NaCl and 0.05 M hematein was used as a redox electrolytic mediator. All measurements were carried out at 20 ± 2 °C.

FT-IR spectra were recorded on a Perkin Elmer SPECTRUM GX-Raman spectrophotometer. ^{1}H NMR spectrum was taken with a Bruker Biospin DRX-600 NMR spectrometer using tetramethylsilane as an internal standard at 25 °C. The weight-average molecular weight (M_w) of PSA and PSSA was determined by size exclusion chromatography (SEC) through a Shodes GPC101 system using LiCl (10 mM) in DMF and THF as eluents, respectively with a flow rate of 1.0 mL/min at 40 °C. The molecular weight was calibrated with polystyrene standards. The electrophoretic mobility of the PSA/PSSA and ABBA containing PSA/PSSA was studied via flat surface cell technique using Beckman Coulter®, Delsa™ PN A54412 ζ-potential analyzer. The ζ-potential was calculated by Smoluchowski relation [27]. The surface morphology of the PSA/PSSA electrospun nanofibers-mat and ABBA containing PSA/PSSA electrospun nanofibers-mat was examined with a JEOL JSM-5600 scanning electron microscope (SEM) operated at 20 kV. The specimens were sputter-coated with a thin layer of platinum (~5 nm) prior to examination. The relative surface hydrophilicity of the PSA/PSSA and ABBA containing PSA/PSSA was measured by automatic research grade contact angle measurement system, Kyowa interface science CA-W using water as liquid phase.

3. Results and discussion

The amphiphilic polyelectrolytes, i.e., PSA and PSSA were synthesized without any surfactant using ultrasound irradiation as shown in Fig. 1 [28]. With influence of ultrasound, the reaction mixture in each case was quickly formed a stable emulsion throughout the reaction. It is found that under ultrasound emulsion polymerization technique, monomer droplets size greatly reduce from the conversional used emulsion polymerization system, i.e., from 2–10 μm to 50–200 nm [25]. Therefore, ultrasound initiated emulsion polymerization methods offer close nucleation locus for hydrophobic droplets during polymerization process. The phenomenon foresees polymeric thermodynamic and structural superior properties that can be described in great detail using density function theory, self-consistent field theory and single-chain mean-field theory [29].

FT-IR spectrum of PSA showed the typical absorption bands at: (i) 3433 (N–H stretching), (ii) 2920 (C–H stretching of aromatic –CH_2 groups), (iii) 2840 (C–H stretching of aliphatic –CH_2 groups), (iv) 1638 (C=O stretching of amide group) and (v) 951, 770, 684 (bending vibrations of C–H groups in the mono benzene ring). Further, ^{1}H NMR of PSA in DMSO-d_6/CD_3Cl was also illustrated characteristic resonances at δ 1.4 (methine proton of polystyrene), δ 1.6 (methylene protons of polyacrylamide main chain), δ 1.8 (methylene protons of polystyrene), δ 2.4 (methine proton of polyacrylamide), δ 6.5 and 7.0 (protons in benzene ring). Thus, both studies confirmed the copolymerization of polystyrene and polyacrylamide. The M_w of PSA copolymer was measured in a range of 163 kDa. In addition, PSSA was also demonstrated the representative FT-IR absorption bands at: (i) 3184 (O–H stretching), (ii) 2929 (C–H stretching of aromatic –CH_2 groups), (iii) 2810 (C–H stretching of aliphatic –CH_2 groups), (iv) 1604 (C–C in-plane stretching of the styrene ring), (v) 1187 (asymmetric stretching vibration of –SO_3 group), (vi) 1039 (symmetric stretching vibration of –SO_3 group), and (vii) 835, 770, 697 (bending vibrations of C–H groups in the mono benzene ring). It is clear that PSSA was formed after polymerization reaction. The M_w of PSSA was calculated in an order of 399 kDa.

In the electrospinning process, the PSA/PSSA nanofibers-mat was extruded under an anode spinneret with the electric force to grounded collector. We have prepared PSA/PSSA nanofibers-mat without beads using PSA (5.8 wt%, M_w 163 kDa) and PSSA (2.9 wt%, M_w 399 kDa) in 1,1,1,3,3,3-hexafluoro-2-propanol/*N*,*N*-dimethylformamide mixture at a fixed voltage, flow rate, humidity and distance from needle to ground, i.e., of 9.3 kV, 0.08 mL/h, <10% and 27 cm, respectively. The prepared PSA/PSSA electrospun nanofibers-mat (cf., mean thickness of ~5 μm) was then used as a substrate for the self-assembling of ABBA (i.e., a weak Lewis acid having capability to form boronate ester with vicinal diols of glucose at the physiological pH) by the physical adsorption technique.

The resultant PSA/PSSA and self-assembled ABBA onto PSA/PSSA electrospun fibers-mats were characterized by FT-IR spectroscopy. Fig. 2a and b shows the FT-IR spectra of the PSA/PSSA and self-assembled ABBA onto PSA/PSSA electrospun fibers-mats. The FT-IR spectrum of the PSA/PSSA electrospun nanofibers-mat (Fig. 2a) showed the characteristic peaks at: (1) 3186–3398 cm^{-1} (O–H and N–H stretching); (2) 2920 and 2844 cm^{-1} (C–H stretching of aromatic and aliphatic –CH_2 groups, respectively); (3) 1658 cm^{-1} (C=O stretching of amide group); (4) 1605 cm^{-1} (C–C in-plane stretching of the styrene ring); (5) 1184 cm^{-1} (asymmetric stretching vibration of –SO_3 group); (6) 1042 cm^{-1} (symmetric stretching vibration of –SO_3 group); and (7) 836 cm^{-1}, 773 cm^{-1}, 670 cm^{-1} (bending vibrations of C–H groups in the mono benzene ring). The characteristic peaks at 1658 cm^{-1} (i.e., C=O stretching of amide

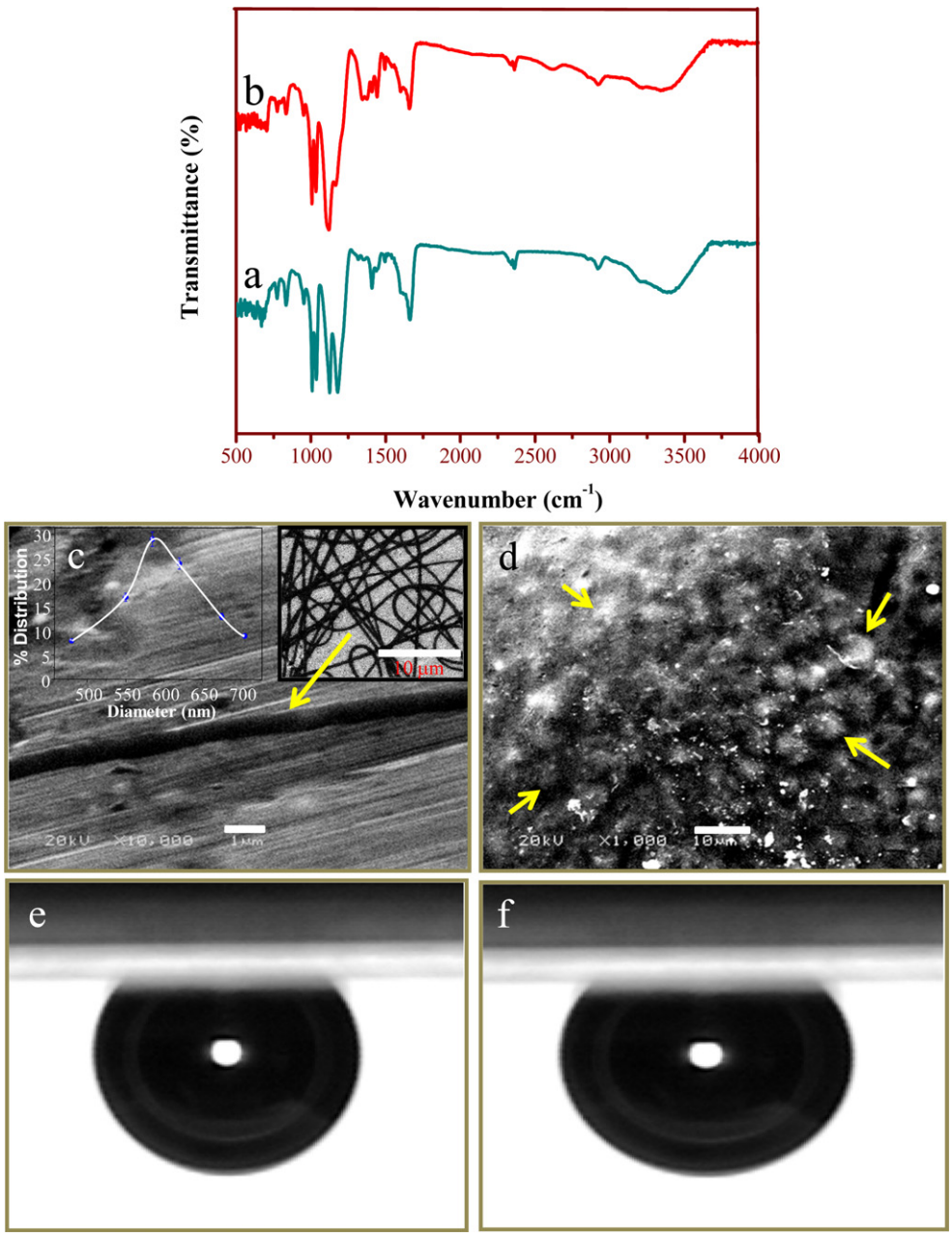

Fig. 2. FT-IR of (a) PSA/PSSA electrospun fiber and (b) self-assembled ABBA containing PSA/PSSA electrospun fibers-mat; SEM micrograph of (c) a PSA/PSSA electrospun nanofiber with a portion of nanofibers-mat (insets: %distribution curve of nanofibers in a nanofibers-mat and an electrospun nanofibers-mat) and (d) ABBA containing PSA/PSSA electrospun nanofibers-mat; image of water bubble on (e) PSA/PSSA surface and (f) ABBA containing PSA/PSSA surface.

group of PSA) and 1184 cm^{-1} (i.e., asymmetric stretching vibration of $-SO_3$ group) confirm the presence of both PSA as well as PSSA in the electrospun fibers-mats. However, ABBA containing PSA/PSSA electrospun nanofibers-mat shows an additional FT-IR absorption peak at 1349 cm^{-1} due to B–O asymmetric stretching of self-assembled ABBA onto PSA/PSSA electrospun nanofibers-mat (Fig. 2b). Hence, FT-IR spectra confirm the self-assembly of ABBA onto PSA/PSSA electrospun nanofibers-mat. Similarly, the ζ-potential measurements of PSA/PSSA electrospun nanofibers-mat before and after adsorption of ABBA, i.e., found to be −64 mV and −82 mV, respectively, attributed that ABBA formed a stable stern layer onto PSA/PSSA electrospun fibers-mat.

A typical SEM picture of PSA/PSSA electrospun nanofibers-mat (Fig. 2c) exhibited tiny fiber networks with the diameter ranging from 480 to 705 nm as shown in insets (cf., % distribution curve of nanofibers in a nanofibers-mat and an electrospun nanofibers-mat). The confined surface of PSA/PSSA electrospun nanofibers-mat is provided a high surface-to-volume ratio, which enhance the accommodation of ABBA upon PSA/PSSA electrospun fibers-mat. It leads to a much higher level of ABBA loading and correspondingly much better detection range for glucose. Self-assembly of ABBA over the PSA/PSSA electrospun nanofibers-mat surface produced a homogeneous globular morphology (Fig. 2d). The uniform globule-like surface may be formed due to the electrostatic binding of ABBA molecules over the amphiphilic PSA/PSSA electrospun nanofibers-mat surface.

To study the relative surface hydrophilicity, the contact angles of PSA/PSSA and self-assembled ABBA onto PSA/PSSA electrospun fibers-mats were measured via captive air bubble method using solid-air bubble-water system and were about 59° and 58.4° (cf.,

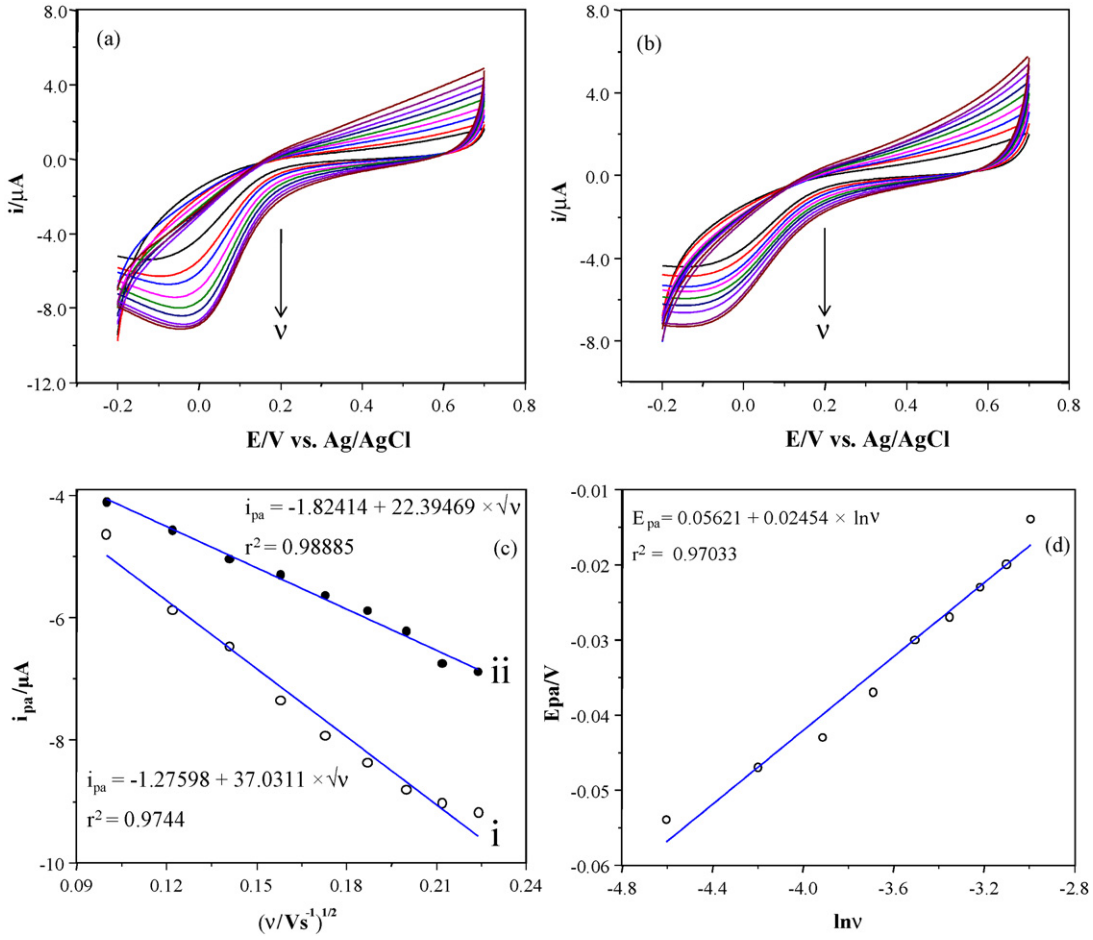

Fig. 3. Cyclic voltammograms of (a) PSA/PSSA electrospun nanofibers-mat electrode; (b) ABBA containing PSA/PSSA electrospun nanofibers-mat electrode; (c) the dependence of the peak current on scan rates; and (d) the relationship between E_{pa} and ln ν of self-assembled ABBA onto PSA/PSSA electrospun nanofibers-mat electrode.

the difference of the measured contact angle of the air bubble from 180°), respectively (Fig. 2e and f). In the solid-air bubble-water system, the increase of the air bubble volume is corresponded to the dewetting of the solid surface and hence water adhesion is higher at a lower contact angle [30]. Since the contact angle slightly decreased after the ABBA self-assembling on the surface of the PSA/PSSA electrospun fibers-mats, this indicates that wettability of ABBA containing PSA/PSSA electrospun nanofibers-mat surface little influenced by adsorbed hydrophilic ABBA moieties.

Fig. 3 shows the cyclic voltammograms of the PSA/PSSA and self-assembled ABBA onto PSA/PSSA electrospun fibers-mats (in 50 mM PBS of pH 7.4 containing 10 mM NaCl, and 0.12 mM hematein) working electrodes at nine different scan rates ranging from 10 to 45 mV s^{-1}. The CV of PSA/PSSA electrospun nanofibers-mat (Fig. 3a) illustrates well-defined electrochemical behavior which accredited to highly charged species on PSA/PSSA mat representing electrons originated from the negatively charged polyelectrolyte medium. It is observed that after self-assembly of ABBA onto PSA/PSSA electrospun fibers-mat, the magnitude of current decreases with lower side potential shift from −37 to −88 mV (Fig. 3b). It may be due to complex ionic pattern of ABBA and PSA/PSSA. This finding supports that ABBA containing PSA/PSSA electrospun nanofibers-mat surface can more easily be reduced compared to bare PSA/PSSA electrospun fibers-mat. The diffusion control process of species to both electrode surfaces, i.e., PSA/PSSA and self-assembled ABBA onto PSA/PSSA electrospun fibers-mats was obtained by plotting reduction peak current (i_{pa}) vs. square root of the scan rate ($\nu^{1/2}$) as shown in Fig. 3c. Here, i_{pa} is proportional to $n^{3/2}D^{1/2}\nu^{1/2}$ at constant surface area of the electrode and analyte's concentration, where, n and D are the number of electrons appearing in half-reaction for the electro-active couple and analyte's diffusion coefficient, respectively. The peak current had a linear response with the scan rate, indicating a diffusion controlled process where the slope of the peak current with the $\nu^{1/2}$, i.e., $di/d\nu^{1/2}$ is proposal to $D^{1/2}$ [31]. The linear regression for both PSA/PSSA and self-assembled ABBA onto PSA/PSSA electrospun fibers-mats electrodes was established:

$$i_{pa} = -1.27598 + 37.0311 \times \nu^{1/2}, \quad r^2 = 0.9744 \tag{1}$$

$$i_{pa} = -1.82414 + 22.39469 \times \nu^{1/2}, \quad r^2 = 0.98885 \tag{2}$$

After self-assembled ABBA onto PSA/PSSA electrospun nanofibers-mat electrode, the slope decreased by a factor of 1.65 compared with that of the PSA/PSSA electrospun nanofibers-mat electrode. This might be due to the physical forces including van der Waal's, coulombic and electrostatic of ABBA with the PSA/PSSA electrospun nanofibers-mat electrode that controls the moment of the supporting electrolyte's/ions.

Using Laviron treatment, the peak potential (E_p) of irreversible adsorption is show a linear relation with ln ν [32]. Fig. 3d was obtained from E_{pa} of self-assembled ABBA onto PSA/PSSA electrospun nanofibers-mat electrode as a function of ln ν. The intercalation mode between ABBA and PSA/PSSA electrospun nanofibers-mat had significantly influence the electrochemical parameters and lead to formation of active super intermolecular ionic complex, which caused the decrease of the i_{pa} with E_{pa} shifting. The shifting of E_{pa} at lower side further supports the

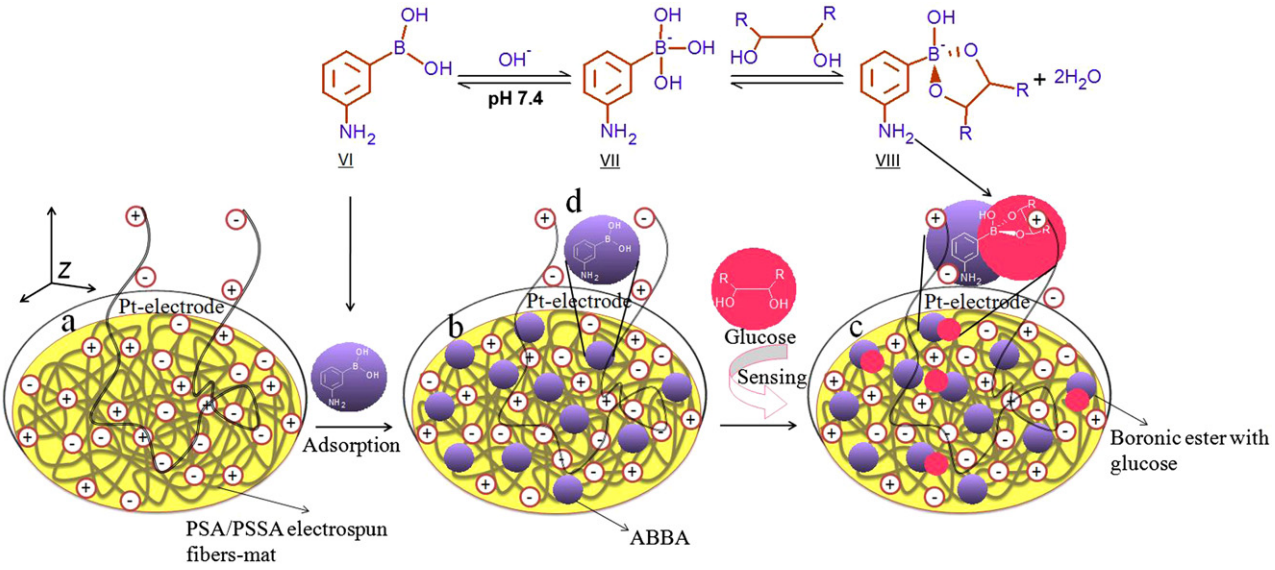

Fig. 4. Schematic diagram of the fabrication process for polyelectrolyte reactor on the Pt-disc electrode: (a) Pt-disc electrode coated with PSA/PSSA electrospun nanofibers-mat, (b) self-assembly of ABBA upon PSA/PSSA electrospun nanofibers-mat, (c) interaction of glucose with ABBA over the electrode surface during glucose sensing, and (d) Formation of boronic ester (VII) via the reaction of 3-aminobenzene boronic acid (VI) and glucose at physiological pH.

faster kinetics of the electron transfer over the PSA/PSSA electrospun nanofibers-mat containing ABBA electrode surface. The linear regression for self-assembled ABBA onto PSA/PSSA electrospun fibers-mats electrodes was obtained:

$$E_{pa} = 0.05621 + 0.02454 \times \ln \nu, \quad r^2 = 0.97033 \tag{3}$$

The surface concentration of self-assembled ABBA upon PSA/PSSA electrospun nanofibers-mat electrode has been estimated using Brown–Anson equation, i.e., $i_{pa} = n^2F^2I^*AV/4RT$, where, i_{pa} is the peak current density in A/cm^2; n is the number of electrons transferred; F is the Faraday constant (96,584 C/mol); I^* surface concentration (mol cm^{-2}) obtain for ABBA containing PSA/PSSA electrospun fibers-mat; A is the surface area of the electrode (1.89 cm^2); V is the scan rate (0.30 V s^{-1}); R is the gas constant (8.314 J/mol K); and T is the absolute temperature (298 K). The value of surface charge concentration was calculated to be 31.38×10^{-2} mol cm^{-2}. I^* usually depends on the electrode material as well as the sensing element immobilization process [33]. I^* of the enzyme-free sensor using self-assembled ABBA onto PSA/PSSA electrospun nanofibers-mat as the electrode is much higher than that of those previously reported glucose sensor (typically $(1.04–3.33) \times 10^{-10}$ mol cm^{-2}) [34]. The high I^* value indicates a high affinity of ABBA to the PSA/PSSA electrospun nanofibers-mat over the electrode surface, which may be attributed to (1) the advantageous polyionic nanoconfined surface of the PSA/PSSA electrospun nanofibers-mat for the self-assembly of ABBA that can favor fast surface reaction, and (2) the high surface-to-volume ratio, which can help to effectively adsorption of ABBA upon PSA/PSSA electrospun fibers-mat. In addition, polyionic nature of PSA/PSSA electrospun nanofibers-mat can provide efficient electron transfer between the active site of the ABBA and the electrode, thereby enhancing the glucose-sensing activity. Therefore, it indicates that self-assembled ABBA containing PSA/PSSA electrospun nanofibers-mat can provide a very high electro-active surface area for the fast glucose sensing. Fig. 4 shows the overall enzyme-free glucose sensor fabrication process that includes (a) deposition of PSA/PSSA electrospun fibers-mat on Pt-disc electrode; (b) self-assembly of ABBA onto PSA/PSSA electrospun fibers-mat; and (c) glucose-recognition.

It is well known that ABBA can preferentially bind with vicinal diols of glucose (only with α-furanose form) via cyclic ester bonds [35]. The reaction of ABBA with diols is illustrated in Fig. 4d. A cyclic boronate ester formation increases the electrophilicity of the boron group that reducing its pK_a value from about 9 to 6. In the presence of glucose at pH 7.4, the ABBA is thus formed ionic derivatives that can accelerate the electrochemical activity of polyionic PSA/PSSA electrospun fibers-mat.

To take advantage of this change of charge, we have designed amperometric enzyme-free glucose-specific sensor. In this respect, the squarewave voltammetry studies were carried out using self-assembled ABBA containing PSA/PSSA electrospun nanofibers-mat electrode. Fig. 5 shows squarewave voltammetry curves obtained as a function of glucose concentration ranging from 0.75 to 14 mM in 50 mM PBS containing 10 mM NaCl as an electrolyte, and 0.12 mM hematein (i.e., a pH-sensitive natural dye) at pH 7.4. It was observed that i_{pa} shifted to a more positive potential as the pH value decreased. The shift in the E_{pa} was approximately 0.9 mV per pH unit. Previous studies indicated the stability of hematein in electro-

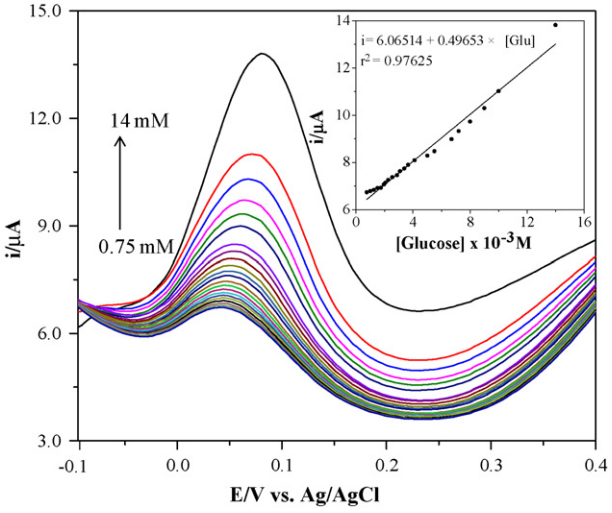

Fig. 5. Squarewave voltammograms obtained from ABBA containing PSA/PSSA electrospun nanofibers-mat electrode as a function of glucose concentration ranging from 0.75 to 14 mM. Inset shows the linear regression curve of the glucose response with ABBA containing PSA/PSSA electrospun nanofibers-mat electrode.

Table 1
Assessment of the ABBA containing PSA/PSSA electrospun nanofibers-mat electrode glucose sensor characteristics with other previously reported boronic acid based glucose sensors.

Sl. no.	Probe materials	Immobilization method	Detection technique	Linear range	Detection limit	Response time	Reference
1	PSA/PSSA electrospun fibers-mat	Physical adsorption	Amperometric	0.75–14 mM	0.75 mM	4 s	Present work
2	Poly(acrylamidophenylboronic acid)-*co*-poly(methyl aminoethyl acrylate)/polystyrene sulfonate polyelectrolyte	–	UV–vis	13.89–27.78 mM	13.89	250 s	[24]
3	Au surface	Physical adsorption	SPR	1×10^{-9}–0.1 mM	1×10^{-9} mM	90 s	[34]
4	9-[*N*-Methyl-*N*-(*o*-boronobenzyl)amino]methyl] anthracene and 9,10-bis[*N*-methyl-*N*-(*o*-boronobenzyl)amino]methyl]-anthracene	–	Fluorescence	0.1–2.5 mM	0.1 mM	–	[36]

chemical cells using Pt composite electrodes depended on both pH and the applied voltage [9]. Accordingly, to avoid electrochemical interference on the stability of hematein, an amperometric measurement of glucose should be conducted at a positive working potential.

The inset of Fig. 5 shows the linear regression curve for enzyme-free sensor response for the glucose concentration ranging from 0.75 to 14 mM onto ABBA containing PSA/PSSA electrospun nanofibers-mat electrode. An amperometric linear response was observed with the successive addition of glucose to the PBS containing 10 mM NaCl as an electrolyte, and 0.12 mM hematein as the redox indicator under a constant stirring at 5-min intervals. The linear regression for glucose response onto PSA/PSSA electrospun nanofibers-mat containing self-assembled ABBA electrode was established:

$$i = 6.06514 + 0.49653 \quad [\text{glucose}], \quad r^2 = 0.97625 \tag{4}$$

The electrode responded within 4 s with successive addition of different glucose concentrations. The current sensitivity of the PSA/PSSA electrospun fibers-mats containing self-assembled ABBA electrode towards glucose concentrations was 0.987 μA/mM cm^{-2}. This new type of enzyme-free glucose sensor demonstrated a shorter response time and a broader diabetic detection range with respect to those reported previously using boronic acid as a glucose-sensing element as shown in Table 1.

The lowest detection limit of the glucose was measured to be 0.75 mM. The reproducibility of the response of the ABBA loaded PSA/PSSA electrospun nanofibers-mat electrode was investigated at a 4.1 mM glucose concentration. No significant decrease in current response was observed after at least 12 uses in testing; thus, the enzyme-free ABBA/PSA/PSSA electrospun nanofibers-mat electrode displayed good reproducibility. The relative standard deviation was found to be about ±6.8%, i.e., determined by five successive measurements of a 4.1 mM glucose standard using a single sensor with the same ABBA/PSA/PSSA electrospun nanofibers-mat electrode. In a series of 12 enzyme-free sensors (cf., using 12 different ABBA/PSA/PSSA electrospun nanofibers-mat electrodes), a relative standard deviation of about ±7.3% was obtained for the individual current response of the same sample (4.1 mM glucose). The good reproducibility observed with this enzyme-free sensor, it may be attributed to the specific and efficient bonding of the ABBA with the glucose moieties at this particular sensory system. The storage stability of the ABBA/PSA/PSSA electrospun nanofibers-mat electrode was amperometrically measured and a similar current response was found after storing more than 12 weeks at room temperature. The effect of interferents was studied on the amperometric responses of the sensor employing the ABBA/PSA/PSSA electrospun nanofibers-mat electrode in the presence of 4.1 mM glucose. The interference effects of fructose, galactose, mannose, urea, L-ascorbic acid, L-proline, L-alanine, DL-malic acid and sodium pyruvate on the amperometric response of ABBA/PSA/PSSA electrospun nanofibers-mat electrode was done as adding these substances into the electrochemical cell at their normal physical concentration, i.e., 0.1 mM. It was observed that the presence of interferents had a relative error of less than ±6.17% in the current measured by the amperometric method; therefore, this enzyme-free ABBA/PSA/PSSA electrospun nanofibers-mat electrode can detect glucose with least interference.

4. Conclusions

The ABBA was self-assembled upon an amphiphilic polyelectrolyte, i.e., PSA/PSSA electrospun nanofibers-mat by physical adsorption method and used for enzyme-free detection of glucose. The glucose-specific enzyme-free assay was employed the ABBA containing polyelectrolyte electrode improved the detection limit up to 14 mM and responded within 4 s. The voltammetric sensitivity of this sensor was measured to be 0.987 μA mM^{-1} cm^{-2}. The most promising features of present enzyme-free glucose sensor are good shelf life, high sensitivity, quick response time and barely affected the interferents. The current efforts aim to use enzyme-free ABBA/PSA/PSSA electrospun nanofibers-mat electrodes to formulate an efficient electrochemical glucose sensor that can rapidly detect glucose from the biological samples viz. tears, urine, blood serum or directly from the blood. The proposed enzyme-free polyelectrolyte system could broadly explore with a more nanoconfined structures like fiber, micelle, particle, brush, etc. for development of complex nanosensory systems to detect biomolecules in a less than nanomolar concentrations.

Acknowledgements

The authors are owed their heartfelt gratitude to the National Institute for Materials Science, Japan for providing infrastructure facility and to the JSPS, JST CREST and MEXT, Japan for generous financial supports to carry out this research.

References

[1] B.J. Hoogwerf, Int. J. Diab. Dev. Countries 25 (2005) 63.
[2] R. Tisch, H. McDevitt, Cell 85 (1996) 291.
[3] N. Dicesare, M.R. Pinto, K.S. Schanze, J.R. Lakowicz, Langmuir 18 (2002) 7785.
[4] Z. Cao, P. Nandhikonda, M.D. Heagy, J. Org. Chem. 74 (2009) 3544.
[5] J. Wang, Chem. Rev. (2008) 814.
[6] M. Pohanka, P. Skladal, J. Appl. Biomed. 6 (2008) 57.

[7] J.N. Camara, J.T. Suri, F.E. Cappuccio, R.A. Wessling, B. Singaram, Tetrahedron Lett. 43 (2002) 1139.
[8] A. Tiwari, S.R. Dhakate, Int. J. Biol. Macromol. 44 (2009) 408.
[9] A. Tiwari, S. Aryal, S. Pilla, S. Gong, Talanta 78 (2009) 1401.
[10] S.K. Shukla, A. Tiwari, G.K. Parashar, A.P. Mishra, G.C. Dubey, Talanta 80 (2009) 565.
[11] A. Tiwari, S. Gong, Talanta 77 (2009) 1217.
[12] A. Tiwari, S. Gong, Electroanalysis 20 (2008) 2119.
[13] A. Tiwari, S. Li, Polym. J. 41 (2009) 726.
[14] A. Tiwari, S. Gong, Electroanalysis 20 (2008) 1775.
[15] A. Riklin, E. Katz, I. Wiliner, A. Stocker, A.F. Bückmann, Nature 376 (1995) 672.
[16] R. Wilson, A.P.F. Turner, Biosens. Bioelectron. 7 (1992) 165.
[17] D.D. Borole, U.R. Kapadi, P.P. Mahulikar, D.G. Hundiwale, Eur. Polym. J. 41 (2005) 2183.
[18] J. Njagi, S. Andreescu, Biosens. Bioelectron. 23 (2007) 168.
[19] X. Cui, G. Liu, Y. Lin, Nanomed.: Nanotechnol. Biol. Med. 1 (2005) 130.
[20] Z. Dai, G. Shao, J. Hong, J. Bao, J. Shen, Biosens. Bioelectron. 24 (2009) 1286.
[21] M.E.M.I. Ekanayake, D.M.G. Preethichandra, K. Kaneto, Biosens. Bioelectron. 23 (2007) 107.
[22] A. Eremenko, I. Kurochkin, S. Chernov, A. Barmin, A. Yaroslavov, T. Moskvitina, Thin Solid Films 260 (1995) 212.
[23] D. Wang, X. Gong, P.S. Heeger, F. Rininsland, G.C. Bazan, A.J. Heeger, Proc. Natl. Acad. Sci. U.S.A. 99 (2002) 49.
[24] B.G.D. Geest, A.M. Jonas, J. Demeester, S.C. De-Smedt, Langmuir 22 (2006) 5070.
[25] L. Yan, J. Ji, D. Xie, W. Li, G. Zhang, Polym. Adv. Technol. 19 (2008) 221.
[26] H. Kobayashi, Y. Yokoyama, C. Yoshikawa, S. Igarashi, S. Hattori, T. Honda, H. Koyama, T. Takato, in: T. Tateishi (Ed.), Biomaterials in Asia, World Scientific Publishing Co., Singapore, 2007, pp. 182–193.
[27] A. Sze, D. Erickson, L. Ren, D. Li, J. Colloid Interf. Sci. 261 (2003) 402.
[28] J.D. Wadhawan, F. Marken, R.G. Compton, Pure Appl. Chem. 73 (2001) 1947.
[29] M.A.C. Stuart, W.T.S. Huck, J. Genzer, M. Muller, C. Ober, M. Stamm, G.B. Sukhorukov, I. Szleifer, V.V. Tsukruk, M. Urban, F. Winnik, S. Zauscher, I. Luzinov, S. Minko, Nat. Mater. 9 (2010) 101.
[30] K. Grundke, T. Bogumil, C. Werner, A. Janke, K. Poschel, H.-J. Jacobasch, Colloids Surf. A: Physicochem. Eng. Aspects 116 (1999) 79.
[31] P.R. Solanki, A.K. Kausik, A.A. Ahamad, A. Tiwari, B.D. Malhotra, Sens. Actuators B 137 (2009) 727.
[32] E. Laviron, J. Electroanal. Chem. 101 (1979) 19.
[33] A. Tiwari, S.K. Shukla, Express Polym. Lett. 3 (2009) 553.
[34] H. Chen, M. Lee, J. Lee, J.-H. Kim, Y.-S. Gal, Y.-H. Hwang, W.G. An, K. Koh, Sensors 7 (2007) 1480.
[35] J.C. Norrild, H. Eggert, J. Am. Chem. Soc. 117 (1995) 1479.
[36] N. DiCesare, J.R. Lakowicz, Anal. Biochem. 294 (2001) 154.